Organic semiconductor materials (OSMs) attract much interest due to their outstanding physicochemical and optoelectronic properties [1], which enable unique characteristics of electronic devices based on them as compared to analogues incorporating inorganic semiconductors. In particular, OSMs such as conjugated polymers or low molecular compounds (small molecules) can be processed from solution by different coating techniques on lightweight, mechanically flexible substrates or even on stretchable textiles [2,3]. Therefore, easy processing along with modulation of properties of OSMs by molecular design allows to fabricate various electronic devices such as organic solar cells [4], organic photodetectors [5,6], and organic field-effect transistors [7] with desired functions. In the last decade, organic semiconductors with conjugated backbone structure have also found application in perovskite solar cells as dopant-free hole- or electron-transport materials [8,9].

The efficiency of organic or hybrid electronics is strongly influenced by the charge carrier mobility of OSMs, which in turn is closely related to their electronic structure, conformation, and molecular ordering in solid state [10]. Charge-transport characteristics of conjugated polymers are usually limited due to their inherently disordered nature resulting in a large number of charge traps [11,12]. In this regard, the small conjugated molecules exhibiting well-defined structure and a high degree of order attract much interest since these advantages are beneficial for efficient transport of the charge carriers [13]. The charge mobility of small molecules can be additionally improved by thermal annealing of films based on them. This approach allows to govern the morphology and increase the crystallinity of thin films through the rearrangement of small molecules [14,15]. Since the transport of charge carriers within the crystalline domains is facilitated, thermal annealing can be considered as a powerful and straightforward tool for enhancing the performance of organic and hybrid electronic devices.

In our previous works, we reported the synthesis of a family of thiophene(T)-benzothiadiazole(B) small molecules with the general formula of TBTBT, which were shown to be promising components of active layer for organic solar cells, p-type semiconductor materials for field-effect transistors [16], and hole-transport materials for perovskite solar cells [17]. Although the performance of devices was limited mainly by moderate charge-transport characteristics of investigated materials.

Herein, we performed a modification of TBTBT compounds in order to explore the impact of the molecular structure of small molecules on their optoelectronic properties, thermal behavior, texture and morphology of thin films, and as a result charge mobility. We used electron-rich thiophene (T), rigid benzodithiophene (BDT) or more flexible1,4-di(thiophen-2-yl)benzene (TPh) moieties as a central linker. Additionally, terminal thiophene rings were functionalized with

tributylsilyl and n-octyl side chains to provide good solubility along with enhanced crystallinity of novel materials in solid state [18], since longer C–Si bond length compared to C−C bond is beneficial to enhance the π−π stacking and planarity of organic semiconductors [19,20].

The BDT-containing compounds were shown to be more promising in terms of tuning the morphology upon thermal treatment. Impressive enhancement of hole mobilities by 51.5 times was found for films based on a compound **M4** comprising triisopropylsilyl functionalized BDT core. These results provide a favorable experience and strategy for rational design and modification of state-of-the-art OSMs.

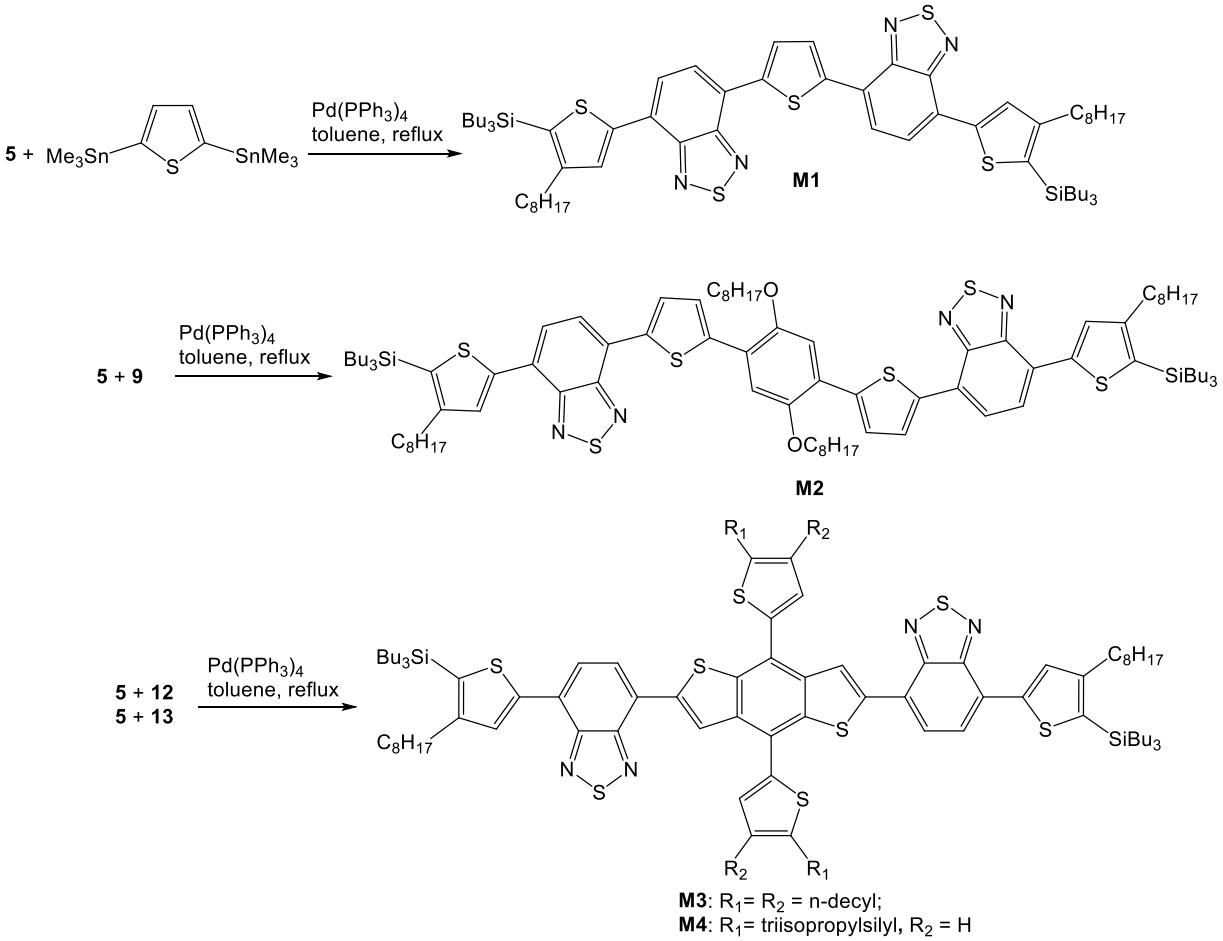

Figure 1. Synthesis of small molecules **M1**-**M4**.

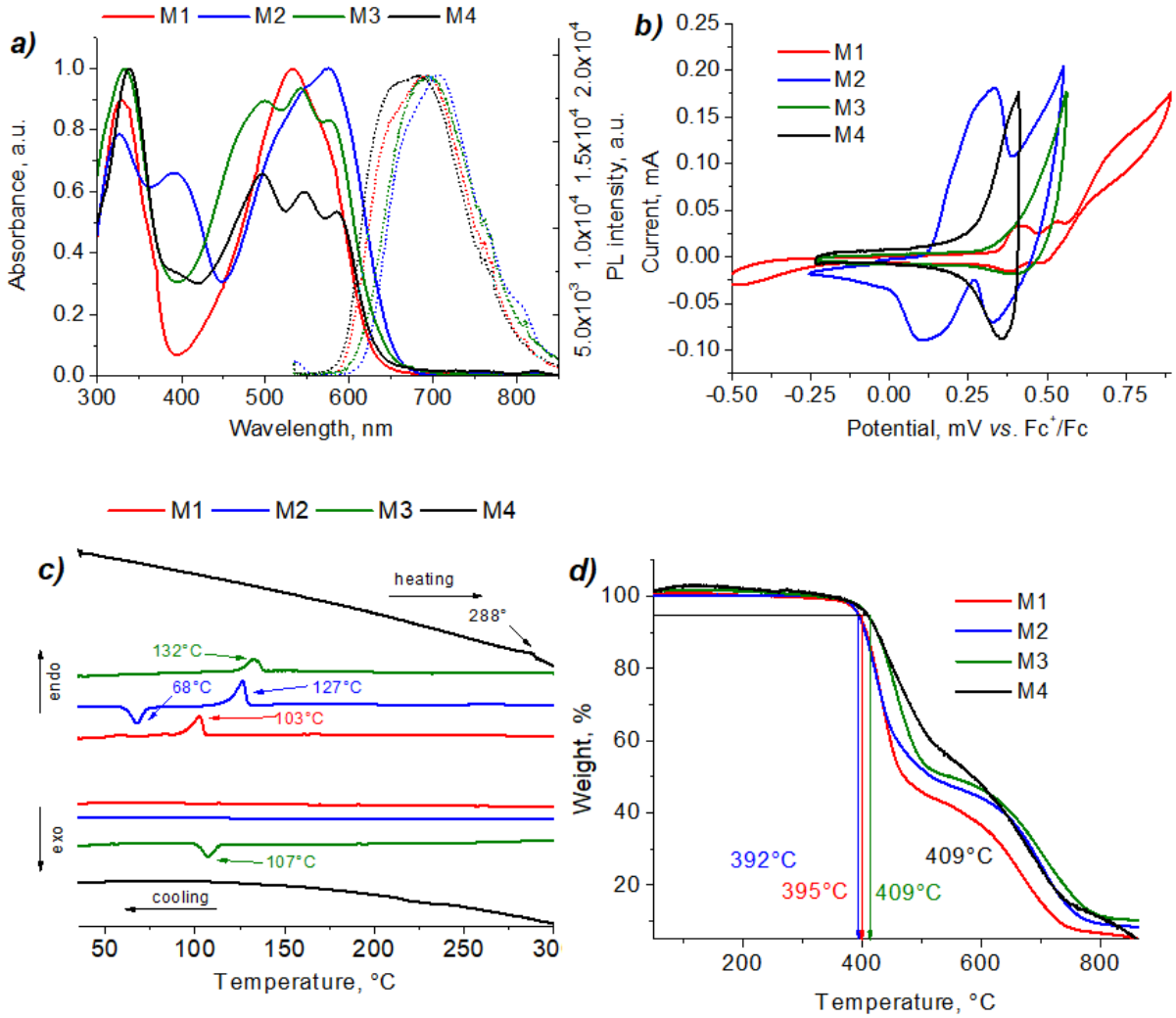

Figure 2. Absorption spectra in solution and thin films of **M1**-**M4** (***a***); CV curves for thin **M1**-**M4** films in 0.1M Bu_4NPF_6 in acetonitrile at scan rate of 50 mV s^{-1} (***b***); DSC thermograms (***c***) and TGA plots (***d***) measured in inert atmosphere.

The energies of frontier molecular orbitals of synthesized small molecules were estimated by cyclic voltammetry. This allows to additionally evaluate the potential of compounds as semiconductor materials for thin-film electronics. The onset of oxidation potentials was extracted from oxidation waves measured for films of corresponding molecules (Figure 1, Table 1). The HOMO energies were calculated as $\mathrm{HOMO} = -e(E_{ox}^{onset} + 4.8)$ eV. It can be clearly seen that HOMO energy levels are influenced by the structure of the central donor block of molecules. The high-lying HOMO level of -4.93 eV was obtained for molecule **M2** consisting of the strong electron-donor thiophene-phenylene-thiophene motif in the backbone, while benzodithiophene-based molecule **M3** exhibited low-lying HOMO energy of -5.19 eV. The LUMO energies were calculated as E_g+E_{HOMO}. The relative positions of frontier energy levels of designed molecules feature them as electron-donor materials for bulk-heterojunction OSCs, since photo-induced charge transfer could be allowed between **M1**-**M4** and state-of-the-art non-fullerene acceptors (Y6, ITIC-4F). Furthermore, small molecules are suitable as hole-transport materials in perovskite

solar cells. The HOMO energies of **M1**-**M4** are well aligned with the valence band of $CH_3NH_3PbI_3$ perovskite absorber material, whereas LUMO energies lie above its conduction band [24] that facilitates efficient hole extraction and blocking the transport of electrons, respectively.

Table 1. Optical, electrochemical and thermal properties of compounds **M1**-**M4**.

	λ_{max}^{abs}, nm	λ_{max}^{PL}, nm	E_g^{opt}, eV	E_{ox}^{onset},V *vs.* Fc^+/Fc	HOMO, eV	LUMO, eV	T_d, °C	T_m/T_c,°C
M1	532	691	1.99	0.34	-5.14	-3.15	395	103/n.a.
M2	575	706	1.90	0.13	-4.93	-3.03	392	68,127/n.a.
M3	497, 542, 579	693	1.96	0.39	-5.19	-3.23	409	132/107
M4	499, 545, 586	682	1.95	0.27	-5.07	-3.12	409	288/n.a.

To get more insight into the morphology of **M1**-**M4** films, grazing incidence wide-angle X-ray scattering (GIWAXS) measurements were carried out before and after annealing of spin-coated films. Figure 3 shows the 2D GIWAXS patterns of as-cast films of **M1**-**M4** and annealed films at 150°C. It is worth noting that the thin ring at all patterns is machine error due to reflection of detector protector film. Surprisingly, the preferential π-π stacking orientation seems absent for all samples. For as-cast **M1** film, four wide reflections at 18.8 Å, 11.6 Å, 6.9 Å and 4.6 Å are found indicating the formation of a small defected crystal phase (Fig.3a). After annealing, one can see only reflection at 4.3Å typical for an inter-chain distance of alkyl side groups [28,29] (Fig.3b).

Thus, the crystallinity of **M1**-based films is damaged after annealing that correlates well with changes in the texture of films revealed by POM. The neat **M2** films showed a diffraction pattern similar to that of **M1** with reflections with d-spacing 17.2 Å, 5.6 Å and 4.5 Å (Fig.3c). However, the crystal structure is recovered after annealing revealing a faster crystallization process that is in agreement with POM data. Crystals remain small and imperfect that suggest a high nucleation rate and low growth rate during crystallization from the melt at room temperature (Fig.3d). For as-cast film of **M3**, GIWAXS patterns show narrow intense reflection at 0.039 $Å^{-1}$ and two broad peaks with d-spacing of 4.6 Å and 3.6 Å (Fig.5e). Such pattern was indexed as smectic liquid crystalline (LC) phase with inter-layer distance a_{sm}=25.6 Å, which is close to length of conjugated backbone of **M3** (approx. 32 Å).

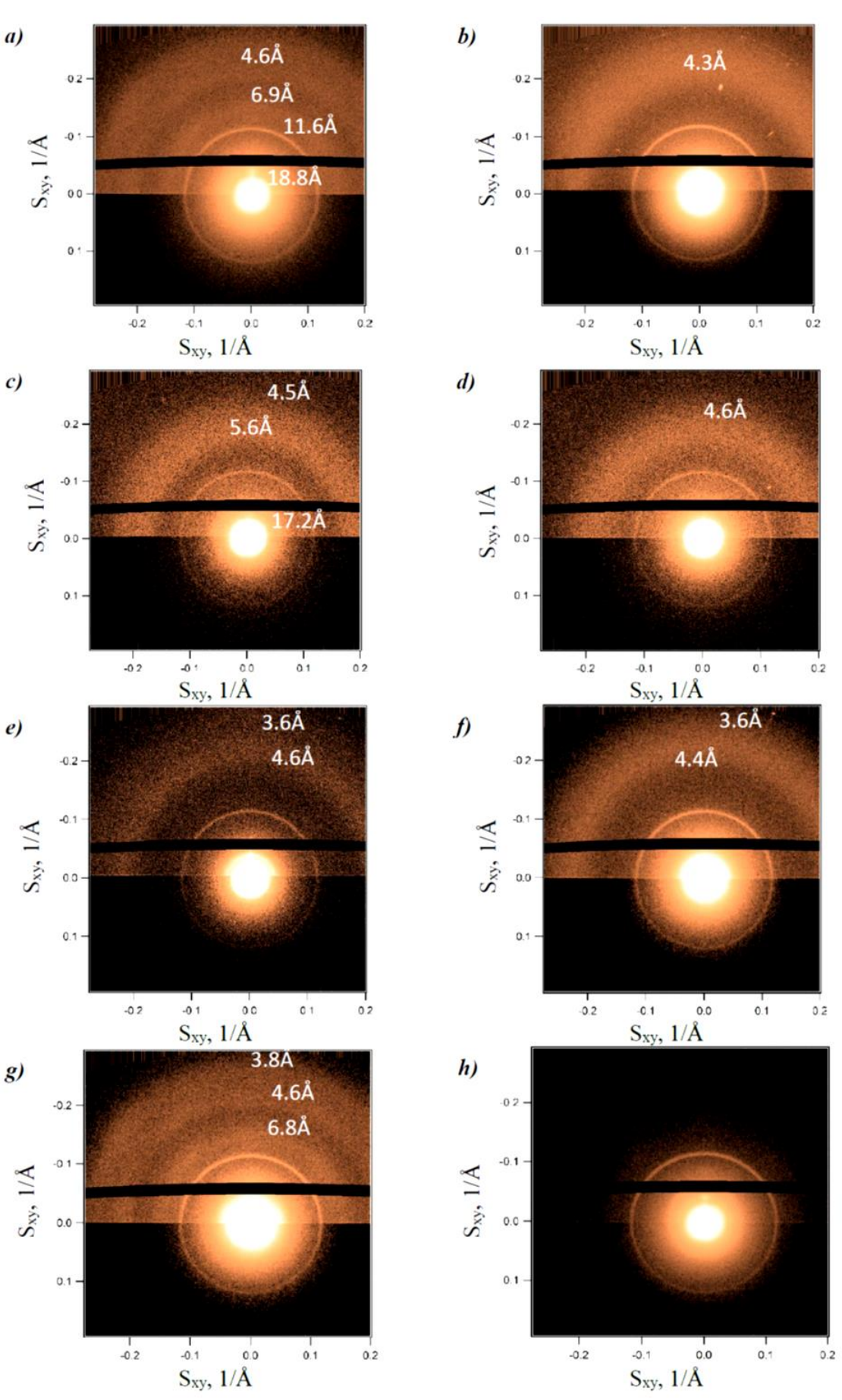

Figure 3. 2D GIWAXS patterns of as-cast **M1**-**M4** films (***a***,***c***,***e***,***g***) and annealed films at 150 °C (***b***,***d***,***f***,***h***)

After annealing of **M3**, the smectic peak shifted to smaller angles resulting in increasing a_{sm} to 26.3 Å along with increasing intensity of reflection at 3.6 Å (Fig. 3f). We suppose that annealing of **M3** at 150°C occurs in an LC state that allows to improve the local ordering of conjugated cores. A similar structure demonstrated the thin film of **M4**. The neat film showed a smectic peak at 0.053 $Å^{-1}$ and oriented crystalline reflections with d-spacing 6.8 Å, 4.6 Å and 3.8 Å (Fig.3g). Annealing in the LC state destroyed the crystalline phase keeping phase-separated smectic morphology (Fig.3h). Such partially-ordered organization formed during processing and post-treatment (deposition method, solvent variation, annealing) can provide larger domains without sharp inter-grain boundaries [30]. Thus, LC active layer could be preferred compared to amorphous or semi-crystalline ones.

Next, we investigated the charge-transport characteristics of small molecules **M1**-**M4** using space-charge limited current method (SCLC) to estimate the impact of structure of small molecules and thermal annealing of thin films on charge mobilities. The hole mobilities were measured in hole-only devices (ITO/PEDOT:PSS/**M1**-**M4**/MoO_3/Ag) with the thin films as-cast and annealed at 150°C The detailed procedure is given in Supporting Information and the results are summarized in **Table** 2.

Table 2. The hole mobilities for hole-only devices based on small molecules **M1**-**M4** before and after annealing

Compound	$\mu_h^{25°C}$, $cm^2V^{-1}s^{-1}$	μ_h^{annl}, $cm^2V^{-1}s^{-1}$	$\mu_h^{annl}/\mu_h^{25°C}$
M1	4.41×10^{-3}	4.24×10^{-4}	0.1
M2	1.27×10^{-3}	2.02×10^{-3}	1.6
M3	1.74×10^{-5}	6.25×10^{-4}	35.9
M4	3.67×10^{-5}	1.89×10^{-3}	51.5

It can be noted that the variation of central electron donor block in small molecules resulted in remarkable changes in hole mobilities measured for as-cast films. **M1** showed highest hole mobility of 4.41×10^{-3} $cm^2V^{-1}s^{-1}$, while μ_h values for benzodithiophene-linked **M3** and **M4** are significantly lower. Replacing of *n*-decyl side chains on BDT unit in **M3** with triisopropylsilyl substituents in **M4** lead to some improving of charge-transport characteristics. As we mentioned above, this fact can be explained by the formation of thin films with liquid-crystalline morphology with phase-separated aliphatic and conjugated blocks. However, higher content of alkyl chains in **M3** promotes stronger phase separation of conjugated and non-conjugated parts that weakens the hole transport.

Thermal treatment of **M1** resulted in a decrease in hole mobility by one order of magnitude. This can be explained by the amorphous disordered morphology of **M1** films that was supported by POM and GIWAXS data. On the contrary, annealed films based on **M2** demonstrated 1.6 times

higher μ_h values due to recrystallization after annealing. The films based on both BDT-containing materials exhibited improved charge transport after annealing. Impressive enhancement in hole mobilities from 3.67×10^{-5} $cm^2V^{-1}s^{-1}$ to 1.89×10^{-3} $cm^2V^{-1}s^{-1}$ was found for **M4**. These is attributed to better ordering of BDT-based molecules in solid state upon annealing, which was also confirmed by wide-angle X-ray scattering technique and POM measurements. Thus, the structure of central donor linker affords critical control over self-ordering of developed molecules in solid state and consequently their semiconductor properties. Despite the fact that thiophene-linked small molecule **M1** exhibited higher hole mobilities, its application in optoelectronic devices operating under realistic conditions (increased temperatures) could result in the deterioration of their performance over time. In this regard, **M2** and benzodithiophene-based compound **M4** have great potential as semiconductor materials for thin-films electronics.

References

[1] Q. Zhang, W. Hu, H. Sirringhaus, K. Müllen, *Adv.Mater*.**2022**, *34*, 2108701.

[2] J. Song, H. Liu, Z. Zhao, P. Lin, F. Yan, *Adv.Mater.* **2023**, 2300034.

[3] X. Wu, W. Fu, H. Chen, *ACS Appl. Polym. Mater.* **2022**, *4*, 4609.

[4] R. Zhou, Z. Jiang, C. Yang, J. Yu, J. Feng, M. A. Adil, D. Deng, W. Zou, J. Zhang, K. Lu, W. Ma, F. Gao, Z. Wei, *Nat. Commun.* **2019**, *10*, 5393.

[5] L. Li, Y. Huang, J. Peng, Y. Cao, X. Peng, *J. Mater. Chem. C* **2014**, *2*, 1372.

[6] C. Lee, R. Estrada, Y. Li, S. Biring, N. R. A. Amin, M. Li, S. Liu, K. Wong, *Adv. Optical Mater.* **2020**, *8*, 2000519.

[7] Y. Yu, Q. Ma, H. Ling, W. Li, R. Ju, L. Bian, N. Shi, Y. Qian, M. Yi, L. Xie, W. Huang, *Adv. Funct. Mater.* **2019**, *29*, 1904602.

[8] A. N. Mikheeva, I. E. Kuznetsov, M. M. Tepliakova, A. Elakshar, M. V. Gapanovich, Y. G. Gladush, E. O. Perepelitsina, M. E. Sideltsev, A. F. Akhkiamova, A. A. Piryazev, A. G. Nasibulin, A. V. Akkuratov, *Molecules* **2022**, *27*, 8333.

[9] A. Rasool, S. Zahid, M. Ans, S. Muhammad, K. Ayub, J. Iqbal, *ACS Omega* **2022**, *7*, 844.

[10] B. Rice, L. M. LeBlanc, A. Otero-de-la-Roza, M. J. Fuchter, E. R. Johnson, J. Nelson, K. E. Jelfs, *Nanoscale* **2018**, *10*, 1865.

[11] S. Fratini, M. Nikolka, A. Salleo, G. Schweicher, H. Sirringhaus, *Nat. Mater.* **2020**, *19*, 491.

[12] Y. Yang, Z. Liu, G. Zhang, X. Zhang, D. Zhang, *Adv. Mater.* **2019**, *31*, 1903104.

[13] B. Kan, M. Li, Q. Zhang, F. Liu, X. Wan, Y. Wang, W. Ni, G. Long, X. Yang, H. Feng, Y. Zuo, M. Zhang, F. Huang, Y. Cao, T. P. Russell, Y. Chen, *J. Am. Chem. Soc.* **2015**, *137*, 3886.

[14] T. Zhang, H. Han, Y. Zou, Y.-C. Lee, H. Oshima, K.-T. Wong, R. J. Holmes, *ACS Appl. Mater. Interfaces* **2017**, *9*, 25418.

[15] X. Liao, R. Lv, L. Chen, Y. Chen, *Phys. Chem. Chem. Phys.* **2017**, *19*, 10581.

[16] D. K. Sagdullina, I. E. Kuznetsov, A. V. Akkuratov, L. I. Kuznetsova, S. I. Troyanov, P. A. Troshin, *Synth. Metals* **2019**, *250*, 7.

[17] M. M. Tepliakova, I. E. Kuznetsov, A. N. Mikheeva, M. E. Sideltsev, A. V. Novikov, A. D. Furasova, R. R. Kapaev, A. A. Piryazev, A. T. Kapasharov, T. A. Pugacheva, S. V. Makarov, K. J. Stevenson, A. V. Akkuratov, *IJMS* **2022**, *23*, 13375.

[18] B. Huang, Y. Cheng, H. Jin, J. Liu, X. Huang, Y. Cui, X. Liao, C. Yang, Z. Ma, L. Chen, *Small* **2021**, *17*, 2104451.

[19] H. Yang, C. Cui, Y. Li, *Acc. Mater. Res.* **2021**, *2*, 986.

[20] W. Xu, M. Zi, M. Zhang, R. Hao, P. Shen, B. Zhao, S. Tan, *Dyes Pigments* **2022**, *197*, 109842.

[21] A. N. Mikheeva, I. E. Kuznetsov, M. M. Tepliakova, A. Elakshar, M. V. Gapanovich, Y. G. Gladush, E. O. Perepelitsina, M. E. Sideltsev, A. F. Akhkiamova, A. A. Piryazev, A. G. Nasibulin, A. V. Akkuratov, *Molecules* **2022**, *27*, 8333.

[22] J. L. Brusso, O. D. Hirst, A. Dadvand, S. Ganesan, F. Cicoira, C. M. Robertson, R. T. Oakley, F. Rosei, D. F. Perepichka, *Chem. Mater.* **2008**, *20*, 2484.

[23] R. Mišicák, M. Novota, M. Weis, M. Cigáň, P. Šiffalovič, P. Nádaždy, J. Kožíšek, J. Kožíšková, M. Pavúk, M. Putala, *Synth. Metals* **2017**, *233*, 1.

[24] Q. He, M. Worku, H. Liu, E. Lochner, A. J. Robb, S. Lteif, J. S. R. Vellore Winfred, K. Hanson, J. B. Schlenoff, B. J. Kim, B. Ma, *Angew. Chem. Int. Ed.* **2021**, *60*, 2485.

[25] A. Honda, S. Kakihara, M. Kawai, T. Takahashi, K. Miyamura, *Crystal Growth & Design* **2021**, *21*, 6223.

[26] Y. Tsujimoto, T. Sakurai, Y. Ono, S. Nagano, S. Seki, *J. Phys. Chem. B* **2019**, *123*, 8325.

[27] K. Ishino, H. Shingai, Y. Hikita, I. Yoshikawa, H. Houjou, K. Iwase, *ACS Omega* **2021**, *6*, 32869.

[28] L. I. Kuznetsova, A. A. Piryazev, D. V. Anokhin, A. V. Mumyatov, D. K. Susarova, D. A. Ivanov, P. A. Troshin, *Org. Electron.* **2018**, *58*, 257.

[29] I. E. Kuznetsov, D. V. Anokhin, A. A. Piryazev, M. E. Sideltsev, A. F. Akhkiamova, A. V. Novikov, V. G. Kurbatov, D. A. Ivanov, A. V. Akkuratov, *Phys. Chem. Chem. Phys.* **2022**, *24*, 16041.

[30] Y. A. Avalos Quiroz, T. Koganezawa, P. Perkhun, E. Barulina, C. M. Ruiz, J. Ackermann, N. Yoshimoto, C. Videlot-Ackermann, *Adv. Elect. Mater.* **2022**, *8*, 2100743.

[31] I. E. Kuznetsov, D. V. Anokhin, A. A. Piryazev, M. E. Sideltsev, A. F. Akhkiamova, A. V. Novikov, V. G. Kurbatov, D. A. Ivanov, A. V. Akkuratov, *Phys. Chem. Chem. Phys.* **2022**, *24*, 16041.

[32] A. N. Mikheeva, I. E. Kuznetsov, M. M. Tepliakova, A. Elakshar, M. V. Gapanovich, Y. G. Gladush, E. O. Perepelitsina, M. E. Sideltsev, A. F. Akhkiamova, A. A. Piryazev, A. G. Nasibulin, A. V. Akkuratov, *Molecules* **2022**, *27*, 8333.

[33] I. E. Kuznetsov, S. L. Nikitenko, P. M. Kuznetsov, N. N. Dremova, P. A. Troshin, A. V. Akkuratov, *Macromol. Rapid Commun.* **2020**, *41*, 2000430.